Average high energy neutron flux distribution in the Quinta subcritical assembly irradiated with deuteron beam of 2.0 GeV energy applying the actinide spectral index method.

Marcin Szuta, Elżbieta Strugalska-Gola

DUZ, **UZ3**

20 październik 2020

Average high energy neutron flux distribution in the Quinta sub-critical assembly irradiated with deuteron beam of 2.0 GeV energy applying the actinide spectral index method.

Outline

NCBJ ŚWIERK

1. Introduction
1.1. Fast neutron fluency measurement methods.

- The amount of neutron induced fissioned (N_{yf}) and neutron captured actinide isotopes (N_{yc}) in the actinide sample of volume V_p can be expressed:
- $$N_{yf} = V_p\, \bar{\phi}\, N\, \bar{\sigma}_f\, t \qquad (1)$$
- $$N_{yc} = V_p\, \bar{\phi}\, N\, \bar{\sigma}_c\, t \qquad (2)$$

Where

V_p - actinide sample volume [cm^3],

$\bar{\Phi}$ - average neutron flux in the place of actinide sample location [$n/cm^2 \cdot s$],

N – number of actinide isotopes in volume unit [cm^{-3}],

$\bar{\sigma}_f$; $\bar{\sigma}_c$ -average microscopic cross section for the reactions (n, f) and (n, γ) respectively [barns],

t - irradiation time [s].

1. Introduction
1.1. Fast neutron fluency measurement methods.

- Two different equations for fissioned (N_{yf}) and captured (N_{yc}) actinide isotopes should give the same average neutron flux value what is a proof for correct measurements:

$$\frac{N_{yf}}{N_{yc}} = \frac{V_p\,\bar{\phi}\,N\,\bar{\sigma}_f\,t}{V_p\,\bar{\phi}\,N\,\bar{\sigma}_c\,t} = \frac{\bar{\sigma}_f}{\bar{\sigma}_c}$$

- This is the spectral index

NCBJ
ŚWIERK

1. Introduction

1.1. Fast neutron fluency measurement methods.

- The fast neutron fluence measurement method consists in utilizing neutron irradiated actinide samples for estimating neutron fluence and average neutron energy inside the volume of samples.
- The idea of the actinide spectral index method is to search the neutron energy (E_d) for the ratio ($\alpha(E_d)$) of fission cross section ($\sigma_f(E_d)$) to capture cross section ($\sigma_c(E_d)$) of the selected actinide isotope from the nuclear data base that is equal to the measured ratio (α_m) of fissioned (N_{yf}) and captured (N_{yc}) actinide isotopes (spectral indexes) [1, 2]:
- $$\alpha(E_d) = \frac{\sigma_f(E_d)}{\sigma_c(E_d)} = \alpha_m = \frac{N_{yf}}{N_{yc}} = \frac{\bar{\sigma}_f}{\bar{\sigma}_c}$$

1. Introduction
1.1. Fast neutron fluency measurement methods.

- It is useful to look closely at the ratios $\alpha = \sigma_f / \sigma_c$ of the capture and fission cross section of the Np-237 isotope.
- The fission/absorption ratios are consistently higher for the fast-neutron spectrum. Thus, in a fast spectrum, actinides are preferentially fissioned, not transmuted into higher actinides.

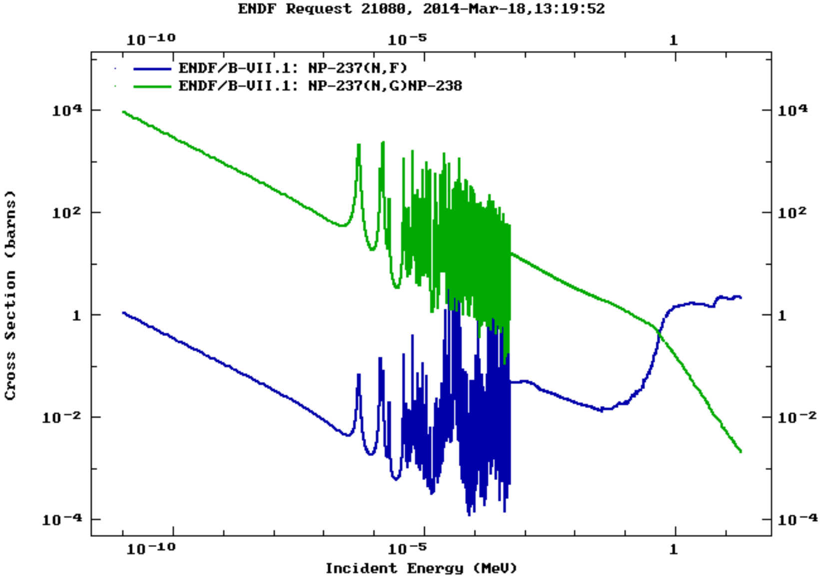

Fig. Cross-sections of Np-237(n,g)Np-238 and Np-237(n,f) reactions.

1. Introduction
1.1. Fast neutron fluency measurement methods.

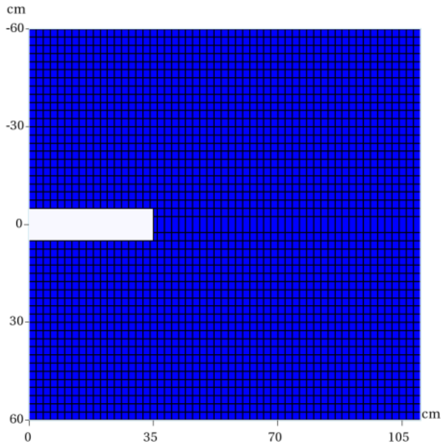

R = 60 cm, L= 110 cm, k_{eff} ~ 0.23

(*V.S. Pronskich et al. // Annals of Nuclear Energy. 2017, v. 109, p. 692-697*)

Neutron spectrum in uranium target
MCNPX, 8 GeV deuterons

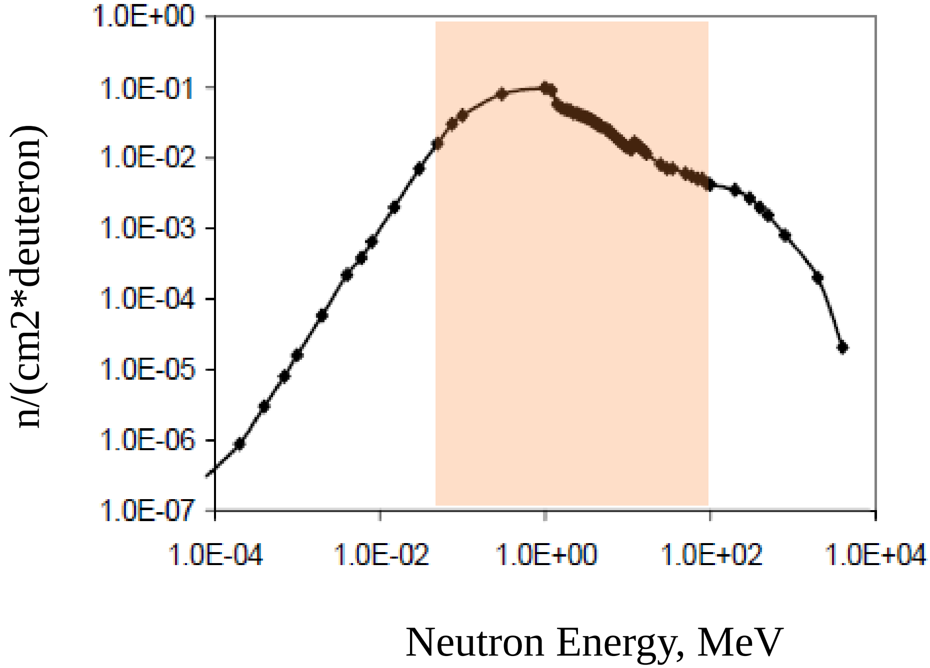

Most of the neutrons in the neutron spectrum generated in the uranium target are concentrated in the energy range from tens of keV to ~ 100 MeV

238U(n,f) – neutron energy > 1 MeV

The neutron spectrum also contains a fast component, which is essential for transmutation via fast fission and other reactions.

1. Introduction

1.1. Fast neutron fluency measurement methods.

Since the measured spectral indexes (α_m) is defined as the ratio of average fission ($\bar{\sigma}_f$) and capture ($\bar{\sigma}_c$) cross sections so the ratio ($\alpha(E_d)$ of retrieved distinct fission ($\sigma_f(E_d)$) and capture ($\sigma_c(E_d)$) cross sections for the distinct neutron energy (E_d) from the nuclear data base describe the average values:

$$E_d = \bar{E}\,;\ \ \sigma_f(E_d) = \bar{\sigma}_f\ ;\ \sigma_c(E_d) = \bar{\sigma}_c$$

Having the average fission and capture cross section values we can evaluate the average neutron flux ($\bar{\phi}$) in the location of the actinide sample using the measured amount of fissioned and captured actinide isotopes.

1. Introduction
1.2. Metallic natural uranium as activation detector foil

- Since metallic natural uranium consists of uranium-238 (99.2752%), uranium-235 (0.7202%), and a very small amount of uranium-234 so the irradiated detector foil introduces an additional error in the measurement of the average neutron flux and neutron fluency.
- Since the measurements of the amount of fissions in the irradiated natural uranium foil constitute the sum of U-238 and U-235 fissions, Eq. (1) must be modified. In contrast, the measurement of neutron captures is based on the measurement of the amount of Pu-239 produced (see Eq.(3)). So the Eq. (2) does not have to be modified since neutron captures are not taken into (considered) account by U-235.
- $$^{238}\mathrm{U}(n,\gamma)^{239}\mathrm{U}\xrightarrow[23.5\,\mathrm{min}]{\beta}{}^{239}\mathrm{Np}\xrightarrow[2.36\mathrm{day}]{\beta}{}^{239}\mathrm{Pu} \qquad (3)$$
- (3)

NCBJ ŚWIERK

1. Introduction
1.2. Metallic natural uranium as activation detector foil

In order to include this we take into account the number of neutron fission induced (N_{yfs}) which is the sum of U-238 (N_{yf8}) and U-235 (N_{yf5}) fissions and neutron captured actinide isotopes (N_{yc8}) in the actinide foil of volume V_p what is expressed by the following equations:

$$N_{yfs} = N_{yf8} + N_{yf5} = V_p\bar{\phi}N_8\bar{\sigma}_{f8}t + V_p\bar{\phi}N_5\bar{\sigma}_{f5}t = V_p\bar{\phi}N_8 t(\bar{\sigma}_{f8} + \frac{N_5}{N_8}\bar{\sigma}_{f5}) \quad (4)$$

$$N_{yc8} = V_p\bar{\phi}N_8\bar{\sigma}_{c8}t \quad (5)$$

Where,

N_8 – number of U-238 atoms in volume unit of actinide foil [cm^{-3}],

N_5 – number of U-235 atoms in volume unit of actinide foil [cm^{-3}],

$\bar{\sigma}_{f8}$ U-238 average microscopic cross section for the reactions (n, f) [barns],

$\bar{\sigma}_{f5}$ U-235 average microscopic cross section for the reactions (n, f) [barns],

$\bar{\sigma}_{c8}$ U-238 average microscopic cross section for the reactions (n, γ) [barns],

$\bar{\Phi}$ - average neutron flux in the place of actinide sample location [$n/cm^2 \cdot s$],

$N_5/ N_8 = 0.7202/99.2752 = 0.00725 = 7.25\ 10^{-3}$

NCBJ ŚWIERK

1. Introduction
1.2. Metallic natural uranium as activation detector foil

The quotient of equations 4 and 5 gives the measured spectral index of the irradiated sample on the left, and on the right we get the expression (α_{m85})which becomes equal to the measured index when we find the neutron energy applying try and error method from the data base for which the relevant fission and capture cross section of the U-238 and U-235 fulfill the equation.

$$\alpha_{m85}(E_d) = \frac{N_{yfs}}{N_{yc8}} = \frac{\bar{\sigma}_{f8}}{\bar{\sigma}_{c8}} + \frac{N_5}{N_8}\frac{\bar{\sigma}_{f5}}{\bar{\sigma}_{c8}} \qquad (6)$$

NCBJ ŚWIERK

1. Introduction
1.2. Metallic natural uranium as activation detector foil

Another words the idea of the method is to search the neutron energy (E_d) for the ratio ($\alpha_{m85}(E_d)$) of fission cross section ($\sigma_{f8}(E_d)$) to capture cross section ($\sigma_{c8}(E_d)$) of the selected actinide isotope U-238 plus the ratio of fission cross section ($\sigma_{f5}(E_d)$) to capture cross section ($\sigma_{c5}(E_d)$) of the selected actinide isotope U-235 multiplied by $N_5/N_8 = 0.7202/99.2752 = 7.25\ 10^{-3}$ from the nuclear data base that is equal to the measured ratio ($\alpha_{m85}(E_d)$) of fissioned (N_{yfs}) and captured (N_{yc8}) actinide isotopes:

$$\alpha_{m85}(E_d) = \frac{N_{yfs}}{N_{yc8}} = \frac{\bar{\sigma}_{f8}}{\bar{\sigma}_{c8}} + 7.25 10^{-3} \frac{\bar{\sigma}_{f5}}{\bar{\sigma}_{c8}} \qquad (7)$$

NCBJ ŚWIERK

2. Experimental part.
2.1. Subcritical assembly Quinta

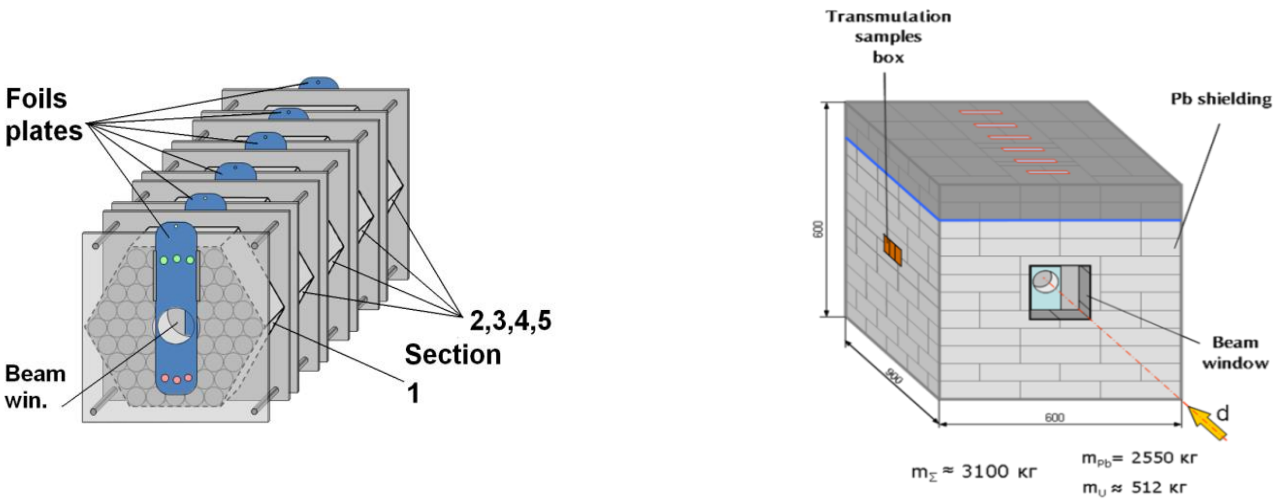

Fig. 1. Schema of Quinta assembly. On the left there is a view on the uranium target with supporting structures and plastics used for sample placement (detector’s plates), on the right there is a view on the lead shielding enfolding the target with marked the transmutation samples box (window) for the actinides sample location in the shielding.

NCBJ
ŚWIERK

2. Experimental part.
2.1. Subcritical assembly Quinta

- Dimensions of Quinta assembly.

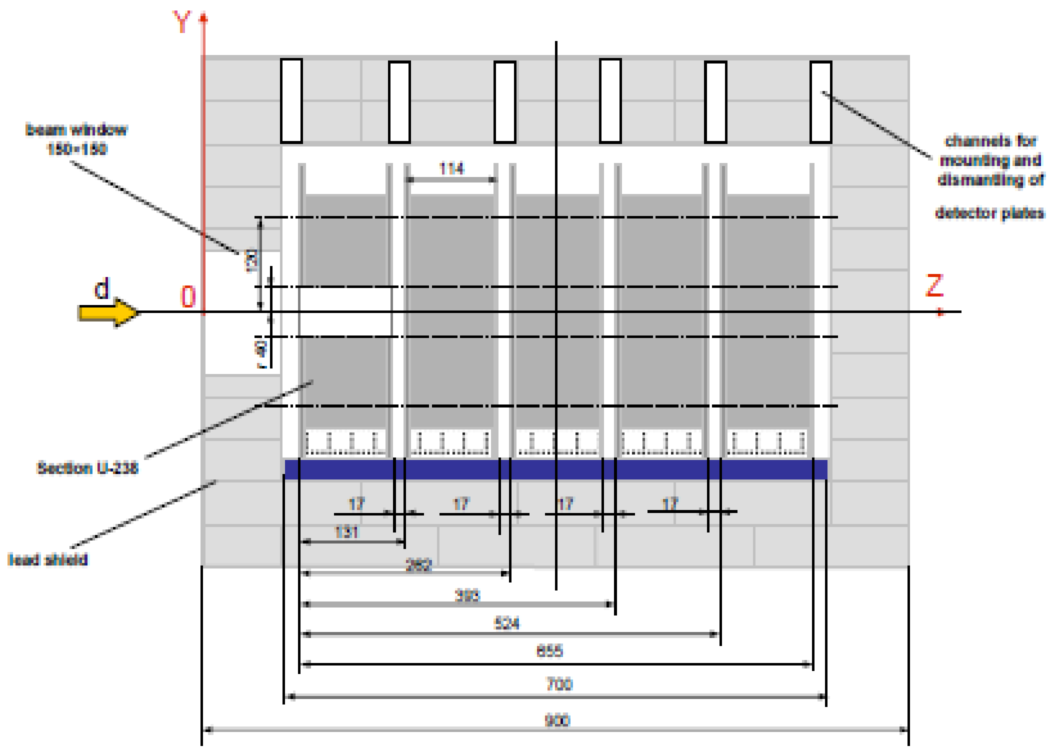

NCBJ
ŚWIERK

2.1. Subcritical assembly Quinta

Sections № 2,3,4,5

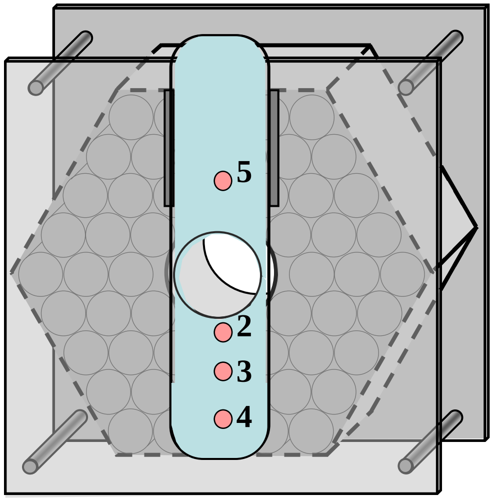

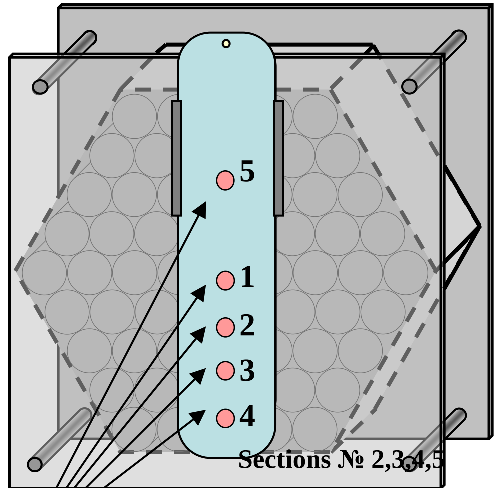

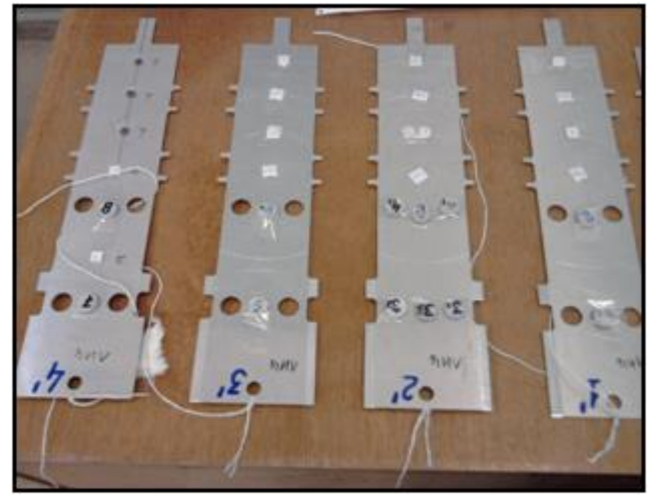

Location of the detectors on the plate

The layout of the uranium foils location on the detector plate. Each plate have 5 positions at the different distances..

- **5** R = -80 mm
- **1** R = 0
- **2** R = 40 mm
- **3** R = 80 mm
- **4** R = 120 mm

Uranium detectors were fixed on the detector plates in dependence on the distance from primary beam axes – 0, 4, 8 and 12 cm.

The dimensions of the foils – diameter 8 mm, thickness 1 mm, weight 1 g.

NCBJ ŚWIERK

2. Experimental part.
2.2. Location of activation detector foils in the Quinta sub-critical assembly.

- The location coordinates of all of 23 uranium detectors are shown in Table 1 relative to the axis of the target (along the radius R of the uranium target and along the axis of the target Z).

Table 1. The location coordinates of all of 23 uranium detectors.

R /Z, mm R - vertically Z - horizontally	**Foil plates**					
	1	*2*	*3*	*4*	*5*	*6*
	0	123	254	385	516	647
0		U_{11}	U_{21}	U_{31}	U_{41}	U_{51}
40	U_{02}	U_{12}	U_{22}	U_{32}	U_{42}	U_{52}
80	U_{03}	U_{13}	U_{23}	U_{33}	U_{43}	U_{53}
120	U_{04}	U_{14}	U_{24}	U_{34}	U_{44}	U_{54}

NCBJ ŚWIERK

2. Experimental part.
2.3. Measurement.
2.3.1. Irradiation details.

- The Quinta target was irradiated with a pulsed deuteron beam of 2.0 GeV energy extracted from the Nuclotron accelerator, located at the JINR.
- Total number of deuterons of the irradiation is equal to 3**.03 $\mathbf{10^{13}}$** during the time of irradiation equal to **22329 seconds (6h 12 min)**.
- Prior to the irradiation, several polaroid films were placed on the front of Quinta to ensure the proton beam was striking in the centre of the beam window.

NCBJ ŚWIERK

2. Experimental part.
2.3. Measurement.
2.3.2. Results

- After the end of irradiation, the uranium foils were taken out from the target to measure γ-spectra using HPGe detectors. Measurement of gamma-ray spectra of irradiated foils was performed in 4 hours after the end of irradiation (more than 10 half-lives of ^{239}U). In this period 99.9% of ^{239}U nuclei have decayed to ^{239}Np.
- The number of fissions was determined by yield of gamma-lines 743.36 keV (93%), 364.49 keV (81.5%), 529.9 keV (87%), and 293.3 keV (42.8%) of fission fragments ^{97}Zr – 5.7%, ^{131}I – 3.6%, ^{133}I – 6.3%, ^{143}Ce – 4.3%. respectively.
- The number of neutron radiation capture reactions was determined by the yield of -line with energy of 277.6 keV γ-line (I=14.44%) accompanying decay of 239Np (see Eq. 3) [3, 4].

NCBJ ŚWIERK

2. Experimental part.
2.3. Measurement.
2.3.2. Results

- The tables below (Table 2 and Table 3,) show the results of measurements of the fission numbers and the number of capture reactions per 1 deuteron and per 1 g of natural uranium.

Table 2. Fission number $Nx10^{-5}$, fiss/g/d

No. Foil plates	*1*	*2*	*3*	*4*	*5*	*6*
R/Z mm	*0*	*123*	*254*	*385*	*516*	*647*
0	0	19.6	33.3	16.1	7.44	2.72
40	1.90	8.53	16.1	9.03	4.89	2.28
80	1.02	4.28	6.83	4.60	2.96	01.57
120	0.85	2.42	3.61	2.72	0.22	0.96

NCBJ ŚWIERK

2. Experimental part.
2.3. Measurement.
2.3.2. Results

- The tables below (Table 2 and Table 3,) show the results of measurements of the fission numbers and the number of capture reactions per 1 deuteron and per 1 g of natural uranium.

Table 3. Capture number, $Nx10^{-5}$, 239Pu/g/d

No. Foil plates	*1*	*2*	*3*	*4*	*5*	*6*
R/Z mm	*0*	*123*	*254*	*385*	*516*	*647*
0	0	8.13	13.77	9.76	5.55	2.34
40	2.53	7.28	12.20	8.51	5.36	2.23
80	1.97	5.74	9.13	6.65	4.41	2.03
120	1.87	4.49	6.02	5.22	3.42	1.76

NCBJ ŚWIERK

2. Experimental part.
2.3. Measurement.
2.3.2. Results

- Having the measured number of fissions and captures in the natural uranium foils we get (obtain) the spectral indexes (see Table 4).

Table 4. Fission to capture ratio – spectral indexes.

No. Foil plates	*1*	*2*	*3*	*4*	*5*	*6*
R/Z mm	*0*	*123*	*254*	*385*	*516*	*647*
0	0	2.411	2.418	1.649	1.341	1.162
40	0.751	1.172	1.319	1.061	0.912	1.022
80	0.518	0.746	0.748	0.692	0.671	0.773
120	0.454	0.539	0.599	0.521	0.561	0.545

2. Experimental part.
2.3. Measurement.
2.3.2. Results

- Having in turn the measured spectral index equal to ratio of average fission and average capture cross section we can evaluate the average neutron flux in the location of the actinide sample using the measured amount of fissioned and captured actinide isotopes.
- This is done by applying the try and error method where we look for the neutron energy for which the ratio of fission cross section to capture cross section of the selected actinide isotope from the nuclear data base is equal to the measured ratio of fissioned and captured actinide isotopes.
- Since the measured ratio is defined as the ratio of average fission and capture cross sections so the retrieved distinct fission and capture cross sections for the distinct neutron energy from the nuclear data base (ENDF/B-VII.1) describe the average values.

NCBJ ŚWIERK

2. Experimental part.
2.3. Measurement.
2.3.2. Results

Table 5. Average neutron energy distribution [MeV].

No. Foil plates	*1*	*2*	*3*	*4*	*5*	*6*
R/Z mm	*0*	*123*	*254*	*385*	*516*	*647*
0	0	1.395	1.396	1.360	1.342	1.329
40	1.298	1.330	1.341	1.322	1.311	1.319
80	1.260	1.297	1.297	1.291	1.288	1.301
120	1.243	1.264	1.277	1.260	1.268	1.266

NCBJ
ŚWIERK

2. Experimental part. 2.3. Measurement. 2.3.2. Results

Fig. 2. Average neutron energy distribution versus target length for four different radiuses.

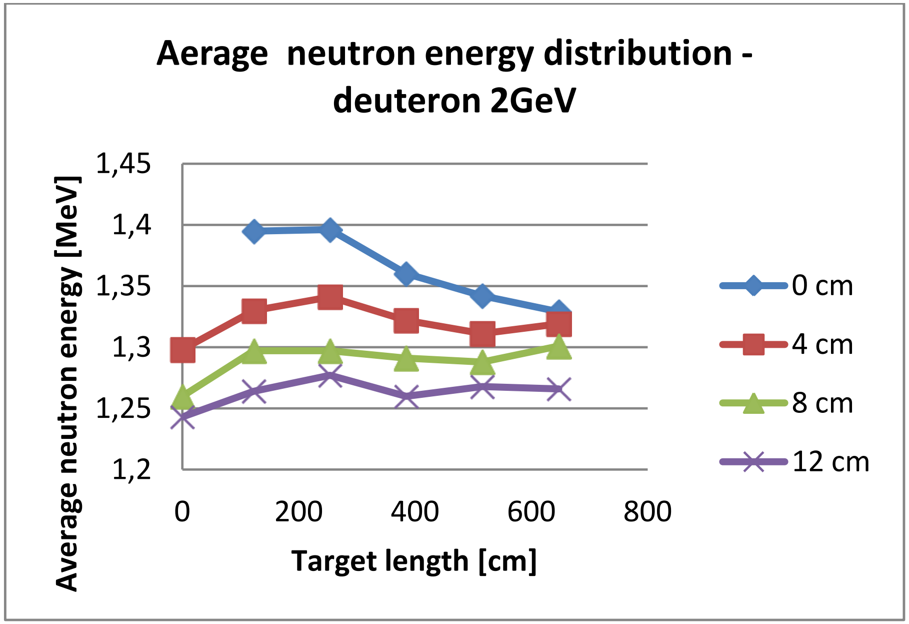

Associating the evaluated average neutron energy (see Table 1 and Fig. 2) with the fission to capture ratio – spectral indexes (Table 4), we can note that the average neutron energy is higher than 1 MeV in all the locations of the detector foils – in whole volume of the Quinta assembly.

2. Experimental part. 2.3. Measurement. 2.3.2. Results

- Course of the charts in Fig. 2 for the average neutron energy in function of target length for different radiuses is to some extent peculiar. While the graph for the radius zero decreases in function of target length, the graphs for higher radiuses (4, 8 and 12 cm) at the beginning increase, then decrease and finally increase again at the end of the target. While the first increase of neutron energy is to some extent understandable, the second increase at the end of target length needs to be explained. This means that some amount of deuterons spread in the target in the form of a cone resulting in an increase in average neutron energy at the end of the target with simultaneous decrease in neutron flux density. In this way, the proportions of neutrons with higher energies relative to lower energies become more pronounced.

NCBJ
ŚWIERK

2. Experimental part.
2.3. Measurement.
2.3.2. Results

Table 6. Average fission and capture cross section distribution for ^{238}U[barn].

No. Foil plates		*1*	*2*	*3*	*4*	*5*	*6*
R/Z mm		*0*	*123*	*254*	*385*	*516*	*647*
0	σ_{f8}	0	0.1834	0.1443	0.1287	0.1044	0.0902
	σ_{c8}	0	0.0804	0.0824	0.0832	0.0846	0.0856
40	σ_{f8}	0.0575	0.0913	0.1033	0.0826	0.0707	0.0794
	σ_{c8}	0.0881	0.0855	0.0847	0.0862	0.0871	0.0864
80	σ_{f8}	0.0385	0.0568	0.0568	0.0530	0.0511	0.0598
	σ_{c8}	0.0911	0.0882	0.0882	0.0886	0.0889	0.0878
120	σ_{f8}	0.0333	0.0400	0.0449	0.0385	0.0419	0.0409
	σ_{c8}	0.0929	0.0908	0.0897	0.0911	0.0904	0.0906

NCBJ
ŚWIERK

2. Experimental part.
2.3. Measurement.
2.3.2. Results

Table 7. Average fission and capture cross section distribution for ^{235}U[barn].

No. Foil plates		*1*	*2*	*3*	*4*	*5*	*6*
R/Z mm		*0*	*123*	*254*	*385*	*516*	*647*
0	σ_{f5}	0	1.2268	1.2269	1.2226	1.2204	1.2189
	σ_{c5}	0	0.0882	0.0882	0.0899	0.0908	0.0914
40	σ_{f5}	1.2151	1.2189	1.2203	1.2180	1.2167	1.2176
	σ_{c5}	0.0930	0.0914	0.0908	0.0917	0.0923	0.0919
80	σ_{f5}	1.2105	1.2150	1.2176	1.2142	1.2139	1.2155
	σ_{c5}	0.0950	0.0930	0.0919	0.0934	0.0935	0.0928
120	σ_{f5}	1.2085	1.2110	1,2126	1.2105	1.2116	1.2112
	σ_{c5}	0.0957	0.0947	0.0941	0.0949	0.0945	0.0946

NCBJ
ŚWIERK

2. Experimental part.
2.3. Measurement.
2.3.2. Results

- The average fission and capture cross sections for ^{238}U[barn] and ^{235}U[barn] presented in Table 6 and Table 7 are corresponding to individual elements of Table 5 in which average neutron energies are given at the location of the natural uranium foils.
- The obtained values for average fission and capture cross sections let us to evaluate the neutron fluencies distribution and average neutron flux distribution in the sub-critical assembly Quinta by help of the equations (Eq. 4 and Eq. 5) . These are collected in Table 8, (Fig. 3) and Table 9 (Fig. 4).

$$N_{yfs} = N_{yf8} + N_{yf5} = V_p \bar{\phi} N_8 \bar{\sigma}_{f8} t + V_p \bar{\phi} N_5 \bar{\sigma}_{f5} t = V_p \bar{\phi} N_8 t (\bar{\sigma}_{f8} + \frac{N_5}{N_8} \bar{\sigma}_{f5}) \quad (4)$$

$$N_{yc8} = V_p \bar{\phi} N_8 \bar{\sigma}_{c8} t \quad (5)$$

NCBJ ŚWIERK

2. Experimental part.
2.3. Measurement.
2.3.2. Results

Table 8. Average neutron flux distribution [x 10^8 cm^{-2} s^{-1}].

No. Foil plates	*1*	*2*	*3*	*4*	*5*	*6*
R/Z mm	*0*	*123*	*254*	*385*	*516*	*647*
0	0	5.426	8.968	6.295	3.520	1.468
40	1.541	4.569	7.730	5.243	3.302	1.385
80	1.158	3.603	5.555	4.028	2.662	1.124
120	1.101	2.653	3.601	3.075	2.030	1.124

NCBJ
ŚWIERK

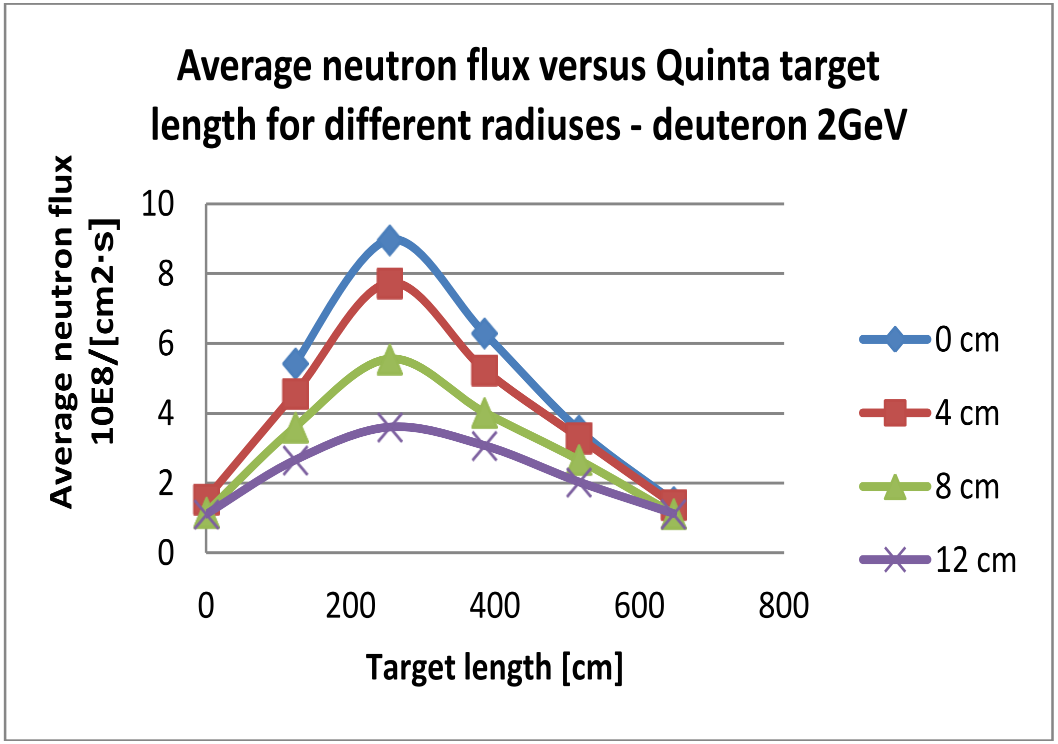

Fig. 3. Average neutron flux distribution versus target length for four different radiuses.

2. Experimental part.
2.3. Measurement.
2.3.2. Results

Table 9. Neutron fluency distribution [x 10^{12} cm^{-2}].

No. Foil plates	*1*	*2*	*3*	*4*	*5*	*6*
R/Z mm	*0*	*123*	*254*	*385*	*516*	*647*
0	0	12.214	20.025	14.057	7.861	3.279
40	3.441	10.203	17.260	11.708	7. 374	3.093
80	2.586	8.045	12.404	8.994	5.944	2.509
120	2.459	5.812	8.042	6.866	4.533	2.465

NCBJ
ŚWIERK

2. Experimental part.
2.3. Measurement.
2.3.2. Results

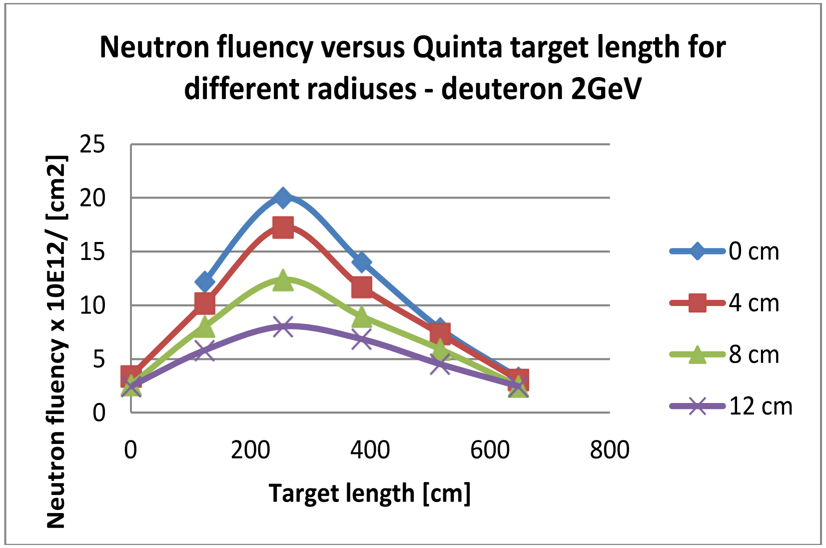

Distribution of 23 natural uranium samples in the whole volume of deeply sub-critical Quinta assembly let us to determine the volumetric distribution of average neutron flux of a specified average energy what in turn it let us to determine the optimal place in the assembly for incineration of the actinide.

So far, such measurements are not performed in the world.

Fig. 4. Neutron fluency distribution versus target length for four different radiuses.

NCBJ
ŚWIERK

3. Estimation of the neutron energy interval significant in the spectral index measurement experiment.

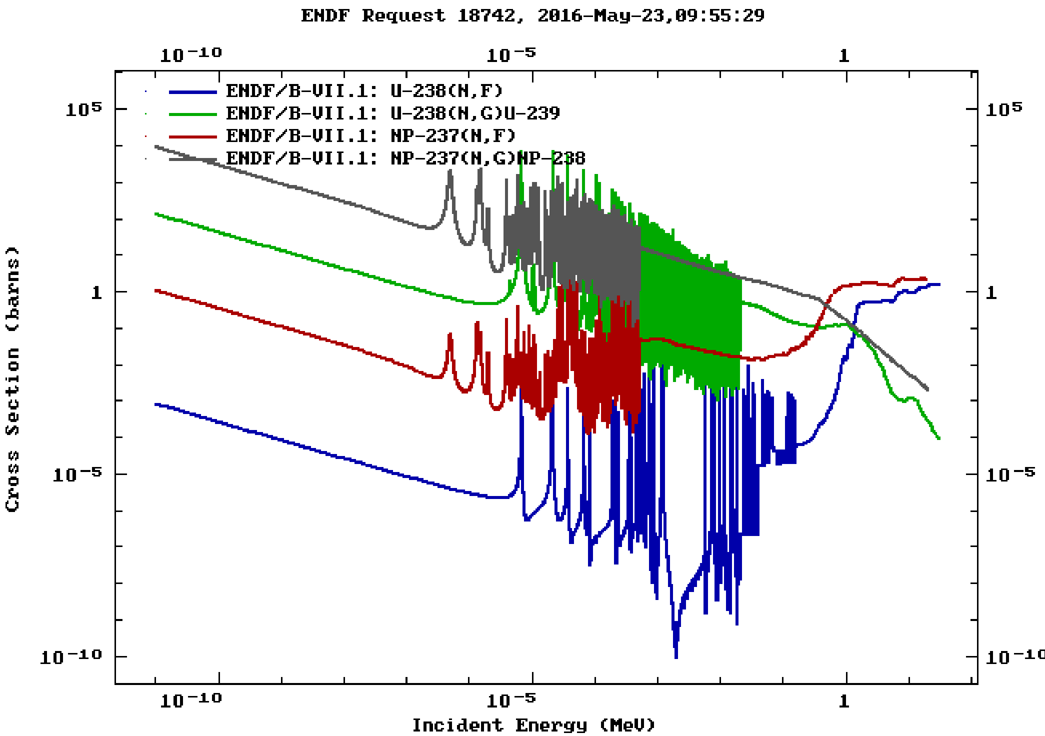

Fig. 5. Fission and capture cross-sections for U-238 and Np-237 versus incident neutron energy.

The fission/absorption ratios are consistently higher for the fast-neutron spectrum. Thus, in a fast spectrum, actinides are preferentially fissioned, not transmuted into higher actinides.

3. Estimation of the neutron energy interval significant in the spectral index measurement experiment.

- The cross-sections of fission and capture as a function of neutron energy of actinides such as U-238 and Np-237 to energy of about 0.1 MeV systematically decreases with the same relation with the predominance of capture.
- In the vicinity of 0.1 - 1 MeV neutron energy, these relationships change in favor of the fission cross section, which after reaching 1-2 bars does not change to about 50 MeV, when the capture cross sections decrease faster.
- Thus, the energy range of 0.1 - 50 MeV is the energy range of neutrons whose average values in this range can be estimated (measured) using the spectral index method provided that we know in advance that the neutron flux density for the smaller energies of 0.1 MeV is negligible.

NCBJ
ŚWIERK

3. Estimation of the neutron energy interval significant in the spectral index measurement experiment.

- The energy range of fission to capture cross sections where their ratio (quotation) is higher than one, just lies in the energy range where the neutron flux is greatest in the Quinta assembly.
- In other words, the logical product of the cross-sectional spectrum for fission and neutron capture and neutron spectrum is a determinant of the neutron energy interval.
- We can accept the criterion that the lower border of the energy interval is when the fission cross section is ten times smaller than the capture cross-section. On the other hand, the upper border of the range (interval) is determined by the energy of the neutron when the fission cross section is larger than the capture cross section.

NCBJ ŚWIERK

3. Estimation of the neutron energy interval significant in the spectral index measurement experiment.

- When analyzing U-238, we obtain that for incident neutron energy Ei equal to 0.93 MeV, the cross-section for fissioning is 0.0154 barn, and the cross-section for capture is 0.124 barn, which can be taken as the lower border of the neutron energy range. This is in line with the (accepted) assumed criterion.
- However the upper border of the neutron energy range in terms of the ratio of fission to capture is not limited by the ratio, but is limited by the neutron flux distribution.
- The magnitude of the neutron flux for neutron energies around 0.07 MeV is about 10 times smaller than the maximum value of the neutron flux density and for the energy of about 2 MeV, the neutron flux density is also about 10 times smaller what we can assume the upper border of neutron energy range.
- So, the neutron energy range 0.07 - 2 MeV of the neutron spectrum is a component which is essential for transmutation of minor actinides [5, 6].

NCBJ
ŚWIERK

3. Estimation of the neutron energy interval significant in the spectral index measurement experiment.

- Considering the spectra of fission and capture, which was previously analyzed, the lower limit of the interesting energy range of neutrons is 0.93 MeV. Ultimately, our range of energy, which is important (decisive) at spectral index measurements is 0.93 - 2.0 MeV.
- The above analysis can be more clearly (better) understood (seen) when applying the Boolean algebra where a Boolean "variable" can have one of the two values, either "1" and "0" . In Table 10 below we distinguished two variables: spectral index (SI) and neutron flux density (NFD) which can get (have, reach) values ("1" or "0") for different ranges of neutron range (NER). The logical product (LP) known commonly as Boolean multiplication produces the multiplied term of the two variables SI and NFD which can also be in the form of a "1" or "0", is a fixed value and therefore cannot change. The LP = 1 if SI = NFD = 1, and LP = 0 otherwise.

NCBJ ŚWIERK

3. Estimation of the neutron energy interval significant in the spectral index measurement experiment.

Table 10. The logical product (LP) of two variables SI and NFD for different ranges of neutron range (NER).

NER (MeV)	< 0.07	0.07 – 0.93	0.93 – 2.0	> 2.0
SI	0	0	1	1
NFD	0	1	1	0
LP	0	0	1	0

Where
NER - neutron energy range
SI is “0” for NE < 0.93 MeV when SI is < 0.1, is “1” for NE > 0.93MeV when SI > 1
NFD is “0” for NE < 0.07 MeV and NE>2.0 MeV when NFD is negligible, is “1” for NE>0.07 MeV and < 2.0 MeV when NFD is considered.

NCBJ ŚWIERK

3. Estimation of the neutron energy interval significant in the spectral index measurement experiment.

- The neutron energy range when the LP value is “1” determines the neutron energy interval significant in the measurement of neutron fluency by the spectral index actinides measurement method.
- Thus, the neutron energy range (0.93 - 2.0 MeV) is the significant range sought for the measurement of neutron fluence by spectral index method.

NCBJ ŚWIERK

4. Conclusions

- Actinide samples can be used as neutron fluency detectors especially in the high neutron energy range that is difficult to measure.
- Both the natural uranium and the neptunium 237 actinides can be applied as high energy neutrons fluencies detectors.
- Since the measurements of fluence of neutrons by the spectral index method using natural uranium and neptunium 237 are quantitatively comparable to some extent, we can conclude that a significant part of the measured fluence of neutrons comes from the neutron energy range 0.9 - 2.0 MeV.

NCBJ ŚWIERK

4. Conclusions

- In the case of irradiation of Am-241 under the conditions described above, the spectral index should reach about 4, which also indicates that the incineration of this actinide will be effective.
- It is widely known that the average neutron energy during the process of fission is about 2 MeV but during the process of spallation is about 3 MeV.
- The quotient of cross sections for fission and capture for these neutron energies (1, 2 and 3 MeV) gives information on incineration of minor actinides. This is clearly seen in Table 10 where are collected the mentioned parameters for these neutron energies extracted from the data base ENDF/B-VII.1.

NCBJ ŚWIERK

4. Conclusions

- The minor-actinide-bearing blanket (MABB) concept [5, 6] is based on irradiation of such blankets containing a significant quantity of minor actinides in a solid solution mixed with uranium oxide which is to be located in radial blankets on the periphery of the outer core in a sodium-cooled fast reactor (SFR).
- Inside in the structure of fuel the average neutron flux can be very close to the average energy of fission neutrons what ensure that the incineration efficiency is within the range of 8 – 27 times higher for Np-237 and 4 - 23 times higher for Am-241 than production of next actinides.

NCBJ
ŚWIERK

5. Referencs

- [1] M. Szuta, S. Kilim, E. Strugalska-Gola, M. Bielewicz, N.I. Zamyatin, A. I Shafronovskaya, S. Tyutyunnikov; Comparison of two fast neutron fluence measurement methods based on Np237 fission to capture ratio measurement (spectral index) and a reverse dark current measurement of planar silicon detector; XXIII International Baldin Seminar on High Energy Physics Problems – "Relativistic Nuclear Physics & Quantum Chromodynamics"; Russia, Dubna, September, 2016.; *Baldin ISHEPP XXIII;* EPJ Web of Conferences **138** 10006 (2017), DOI: 10.1051/epjconf/201713810006
- [2] M. Szuta, S. Kilim, E. Strugalska-Gola, M. Bielewicz, N.I. Zamyatin, A. I Shafronovskaia, S. Tyutyunnikov; Impact of average neutron energy on the fast neutron fluency measurement by Np237 fission to capture ratio and reverse dark current of planar silicon detector methods.;XXIV International Baldin Seminar on High Energy Physics Problems – "Relativistic Nuclear Physics & Quantum Chromodynamics"; Russia, Dubna, September, 2018 *Baldin ISHEPP XXIV;* EPJ Web of Conferences **204**, 0 (2019) https://doi.org/10.1051/epjconf /201920404002
- [3] M.Yu. Artiushenko, V.A. Voronko, K.V. Husak, M.G. Kadykov, Yu.T. Petrusenko, V.V. Sotnikov, D.A. Irzhevskyi, S.I. Tyutyunnikov, W.I. Furman, V.V. Chilap; Investigation of the spatial and energy distributions of neutrons in the massive uranium target irradiated by deuterons with energy of 1…8 GeV; *ISSN 1562-6016. ВАНТ. 2013. №6(88)* 170 - 174
- [4] M.Yu. Artiushenko, A.A. Baldin, A.I. Berlev, V.V. Chilap, O. Dalkhajav, V.V. Sotnikov, S.I. Tyutyunnikov, V.A. Voronk1, A.A. Zhadan**;** Comparison of neutron-physical characterictics of uranium target of assembly „QUINTA" irradiated by relativistic deuterons and ^{12}Cnuclei**;** ISSN 1562-6016. ВАНТ. 2016. №3(103)

5. References.

- [5] B. Valentin, H. Palancher, C. Yver, V. Garat, S. Massara, “Heterogeneous Minor Actinide Transmutation on a UO2 blanket and on (U,Pu)O2 fuel in a SFR – Preliminary design of pin and assembly”, Proc. Int. Conf. GLOBAL 2009, Paris, France, Sept. 6-11, 2009.
- [6] Syriac BEJAOUI, Elio D’AGATA, Ralph HANIA, Thierry LAMBERT, Stéphane BENDOTTI, Cédric NEYROUD, Nathalie HERLET, Jean-Marc BONNEROT ; Americium-Bearing Blanket Separate-effect Experiments:MARIOS and DIAMINO Irradiations; Proceedings of GLOBAL 2011 Makuhari, Japan, Dec. 11-16, 2011 Paper No. 503621

NCBJ ŚWIERK

- Thank you for the attention.

NCBJ
ŚWIERK